OBSERVATION OF EXTENSIVE MASS MOVEMENTS IN THE LIPICA II QUARRY WITH AN EL BEAM DISPLACEMENT SENSOR

OPAZOVANJE OBSEŽNIH PREMIKOV MASE V KAMNOLOMU LIPICA II S SENZORJEM PREMIKA ŽARKA EL

Danijela Ignjatović Stupar
International Space University
67400 Illkirch-Graffenstaden, France
E-mail: danijela.stupar@isunet.edu

Andrej Kos
Marmor Sežana d.d
6210 Sežana, Slovenia
E-mail: kos@marmorsezana.com

Milivoj Vulić
University of Ljubljana,
Faculty of Natural Sciences and Engineering
Aškerčeva cesta 12, 1000 Ljubljana, Slovenia
E-mail: milivoj.vulic@guest.arnes.si

DOI https://doi.org/10.18690/actageotechslov.17.1.23-32.2020

Keywords

natural stone quarry, stability assessment, high safety pillar, rock mass, EL Beam, ARIMA

Ključne besede

kamnolom iz naravnega kamna, ocena stabilnosti, visok varnostni steber, kamnita masa, EL žarek, ARIMA

Abstract

It is not only that humans are playing with the environment, giving the quarry a bad external image, nature also returns a blow into the internal mass movements by decreasing the safety parameters of the room-and-pillar excavation. This paper presents the analytical methods used to observe the individual parameters in the context of monitoring the safety pillars and the deformation of the discontinuities in the underground excavation in the Lipica II natural stone mine. To monitor movements and deformations, the EL-beam gauges are installed on the surface of the safety pillars. The observations used in this case study are represented by two vertical EL-beam displacement measurements, acting as one year-long time series. Using ARMA modelling, we analysed the differences between the measured and predicted values of El-beam displacements. The obtained predictions of the displacements, their negligible effect on the measurements themselves, and the absence of any trends in the calculated differences, proves the feasibility of the applied prediction model.

A longer observation period would allow predictions of possible seasonal characteristics of the time series, while the development of the automatic responding monitoring system, triggered by the warning events, will improve the reporting system for the sudden changes in the smoothness of the predicted values.

Izvleček

Ne samo, da se ljudje igrajo z okoljem, ki daje kamnolomu slabo zunanjo podobo, narava tudi vrača udarec v gibanja notranjih mas z zmanjšanjem varnostnih parametrov izkopavanja prostora in stebrov. V prispevku so predstavljene analitične metode za opazovanje posameznih parametrov v okviru spremljanja varnostnih stebrov in deformacije diskontinuitet v podzemnem izkopu v rudniku naravnega kamna Lipica II. Za spremljanje premikov in deformacij so merilniki žarkov EL nameščeni na površini varnostnih stebrov. Opazovalnici, uporabljeni v tej študiji primera, predstavljata dve navpični meritvi premika snopa EL, ki delujeta kot enoletno časovno vrsto. S pomočjo ARMA modeliranja so bile analizirane razlike med izmerjenimi in predvidenimi vrednostmi premikov El-snopa. Pridobljene napovedi premikov, njihov zanemarljiv učinek na same meritve in odsotnost trendov izračunanih razlik dokazujejo izvedljivost uporabljenega modela napovedovanja.

Daljše obdobje opazovanja bi omogočilo napovedi možnih sezonskih značilnosti časovne serije, medtem ko bo razvoj sistema samodejnega odzivanja za spremljanje, ki ga sprožijo opozorilni dogodki, izboljšal sistem poročanja za nenadne spremembe v gladkosti predvidenih vrednosti.

1 INTRODUCTION

Progressive paleogeographic differentiation, which started in the Santonian and later in the Campanian, has already strongly influenced the sedimentary environments of the Adriatic-Dinaric region. This phenomenon was later followed into the Maastrichtian and Paleogene platform. The subaerial transition of this part of the platform induced palaeokarstification of the limestone sedimentation of the Lipica formation, with the deposition of the carbonates in the Karst region (Fig. 1). In this way, the new magasequence in the formation of the Liburnia and "alveolidic-nummulitic limestone" was begun [1, 2].

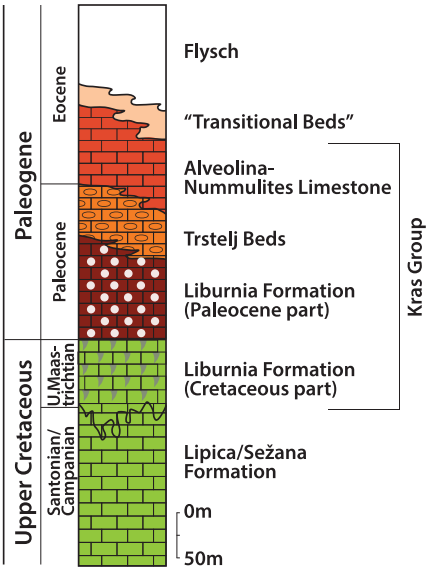

Figure 1. Geological Upper Cretaceous Eocene succession in the Kras (Karst) [2].

Because of its massive structure and uniform texture, this limestone is economically the most important part of carbonate rocks of the classic Karst area. The topography of the Karst region is extremely shallow and skeletal; therefore, the natural recuperation in the case of excavation of the natural stone in the quarries is extremely difficult to control.

The Lipica II quarry (Fig. 2) is one of the successful examples of quarries of natural stone in Slovenia [3]. It represents a progressive spontaneous pollute, although it is made completely of bare rocks. Due to slow leavening, the quarry is still visible as an environmental sore. Nevertheless, it turned out that with the exploitation plan itself, the relief of the affected land can be regulated in an acceptable form.

Figure 2. Lipica II quarry.

The company Marmor Sežana d.d. has been excavating "Lipica Unito" natural stone from the Lipica II quarry since 1986 [4]. Extraction is performed by the room-and--pillar mining method, which is adapted directly on the site (Fig.3). The so-called "room-and-pillar" is a special

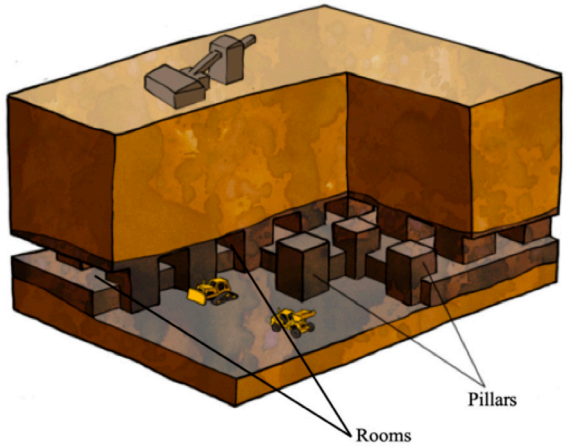

Figure 3. The rooms and pillars mining methodology at Lipica II (top) and room-and-pillar method layout (bottom) [5].

method of mining, where the stone is excavated across a horizontal plane, thus creating horizontal networks between the rooms. In this system rooms/galleries represent the "ore" part, while the pillars are unrestrained materials left out to support the overload of the rooms/galleries' roof. The advantage of the pillars is that their presence reduces the risk of potential subsidence.

Subsidence is one of the main occurrences above underground mining. It has huge impact on the environmental surroundings [6]. Regarding a more natural impact from, but also vice-versa on, the quarry itself, the tree roots can grow deeper through rock cracks and make dissolution on the karst features. This study was used in a limestone quarry in northern Mexico [7].

Other research was dedicated to air pollution near the quarry. The results showed that the concentration of suspended particulate matter (SPM) emissions are 360 $\mu g.m^{-3}$ in the work zone, which is less than 130 $\mu g.m^{-3}$ beyond the site boundary [8]. Taking this impact into consideration, it is recommended to design a green belt around the quarry to decrease the influence on the air quality.

Due to those consequences, before any mine site is opened, jointly with the mine excavation planning, the rehabilitation program of the quarry has to be involved in the mine planning system. This procedure has already been successfully applied in nine limestone quarries. The rehabilitation covers six programs, split into three categories, such as planning, operational, and plan-do--check-act management [9]. The suggested procedure, which was already used in several quarries, could be a good analytical proposal for an environmental recovery solution for Sežana's quarries.

2 MATERIALS AND METHODS

2.1 Materials

The room-and-pillar method layout has to be mapped carefully before the excavation starts. The calculation which determines the important elements of this type of underground mining is a very complex procedure. Geological and geotechnical analyses of a future mining site are introduced through environmental observations. Their results provide an appropriate landmark of the exact methodology that has to be applied in the choice of the mining methodology. The results also define the parameters of the type of tools, machines, and technology which will be used in the excavation. According to the obtained results, the shape and size of the pillars, likewise their position in the mine, are consolidated.

From the mechanical point of view, the excavation procedure for mining natural stone traditionally uses a combined drilling-and-cutting method with the diamond wire and chain cutting machine that is introduced in Fig. 4.

Figure 4. Dimond wire and chain cutting machine.

Prior to the onset of the underground mining, numerical modelling and a calculation of the stability of the predicted underground spaces was performed using the Finite-Difference Method ($FLAC^{2D}$). The $FLAC^{2D}$ model assesses the overall stability of the planned openings and acquires a sensitivity analysis of the input parameters, such as the mechanical characteristics of the rock, including its primary stress, likewise the dimensions and the shape of the mine rooms [3]. The results obtained using these calculations ultimately form the basic design elements of the underground mining site (the rooms and the pillars) and a crucial overview of the selection of a mining method for the long-term extraction of natural stone blocks. Prior to the high safety pillars (HSP) plan making and designing an introduction to determine the largest span of the rooms has to be calculated. This represents the distance between the HSPs and depends on the geomechanical

rock's properties, the geological properties of the site (primary tectonics properties), and the loaf celling, which was overloaded by the arch. Increasing the span, the stability of the ceiling decreases. For that reason it is extremely important to determine the width and the height dimensions of the open spaces (the rooms) and, obviously, the high pillars safety [10, 11].

One of the faster and more visual methods is based on using a terrestrial handhold scanner. Terrestrial Laser Scanning (TLS) makes it possible to collect dense point clouds, representing a visual interpretation of the underground mine rooms and the pillars together. To complete the geolocalization of the observed point cloud, a set of reference points is accurately established on the walls. The first step of the photointerpretation of the geometric characteristics of the mine is cleaning from the unnecessary features (e.g., working equipment, vehicles, cables, etc.). From this mesh, the subsequent 3D topographic maps and orthorectified models are conducted [12].

As already mentioned above, the dimensions of the rooms depend on the geological condition and the mining technology being applied. For instance, in case of Lipica II, the heights of the mining levels range between 4 m and 6 m. Kortnik in [13] provided a numerical analysis based on the geo-mechanical properties of the compact limestone and came up with a model where galleries-rooms with different widths (13 m, 15 m or 20 m) are stable up to a width-to-height ratio of $r = 0.28$. He also estimated that the portal portion of the pillar (the periductular cross section to the surface levels) has to be greater than 13 m.

Named "unwedge", it is yet another block analysis mainly conducted during the excavation. It is focused on the underground block stability structures, followed indirectly by follow-up monitoring of the relative deformations of the discontinuities (stone cracks). A study of a micro fracture network of open cracks could help to better understand the tectonic constraints and to distinguish the origins of the fractures (mechanic or tectonic) [14].

Kortnik in [13], in addition to an analytical calculation and numerical modelling, also provided in-situ data of the stress state and strain measurements of the Lipica II safety pillars. He monitored the behaviour of "safety pillars and rooms" ceilings for a period of 2 years (from 2010 to 2012). The case studies considered the safety pillars SP02 and SP04. The in-situ control measurements were used for monitoring the main stress in a single vertical plane (for the safety pillar SP02), likewise the observation of the temperature. These changes were monitored with a 2D VW stress meter (Model 4350 Vibrating Wire), (Fig. 5).

Figure 5. Biaxial stress meters (VW) [15].

The vertical strains (lateral displacement) were measured with vertical EL beam sensors. The horizontal EL beam sensors monitor the horizontal movement to determine the displacement of the open dikes (Fig. 6).

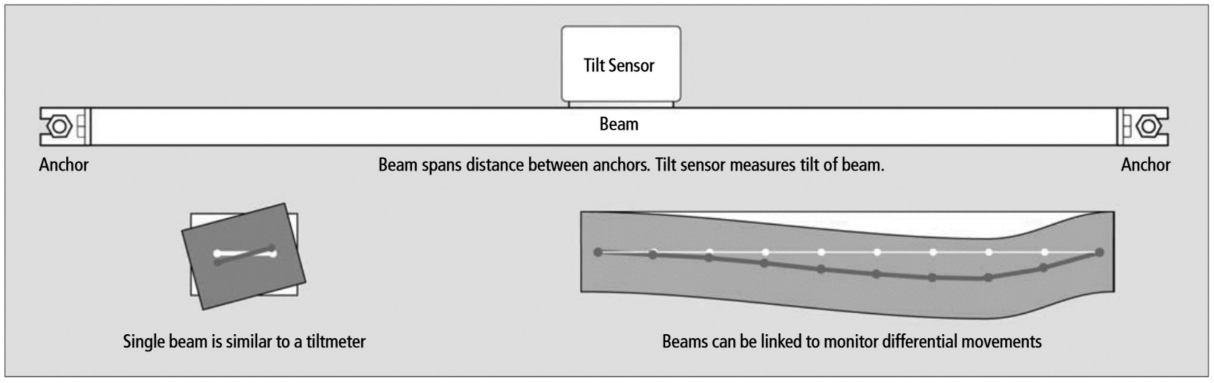

Figure 6. beam sensor [16].

Figure 7. Different types of pillar discontinuities.

In addition, a dike-displacement meter was used as a third option to manually measure the displacements between at least three screws installed along a crack (Fig. 7).

Comparing the numerical model with the in-situ measurements for SP02, Kortnik found congruent results between them.

2.2 Methods

To ensure the stability of the underground galleries, self-supporting stones named high safety pillars are established directly during the stone excavation. Unfortunately, those pillars are exposed to natural extensive mass movements, and for that reason they intersect with many discontinuities. Depending on the types of cracks (Fig. 8), the deformation characteristics and the strength of the rock, the reinforcement requirements are defined. For their definition it is necessary to continuously monitor the safety pillars and, in that way, to detect failures on time, which will allow the mining engineers to react properly with the protection of miners and equipment equally.

There are other techniques that were used for geo--mechanical applications.

One of the experiments was conducted in a quarry in southern Switzerland using 3-axis ground-penetrating radar (georadar) to monitor a quarry's floor [18]. It has been concluded through collected results that the estimation of the quality of the rock can be easily made by using georadar in the observation of excavated or yet to be cut stone. This method could also be used to predict future possible room and pillars cracks and to avoid a possible quarry collapse.

At the Lipica II quarry, the procedure of deformation monitoring has already been applied for many years. There are two established types of monitoring pillar wedges stability:

- using a screw open fissures displacement meter in combination with a glass fissures displacement seal (Fig. 7), and
- monitoring using electronic level (EL) beam gauges.

The latter is focused on voltage conditions in high security pillars, observed by bi-axial stress-meters (vibrating wire sensor). To monitor the movements and deformations, EL-beam gauges are installed on the surface of the safety pillars. The EL beam looks like a bar strain gauge tilt sensor, metal rod, 1.5 to 6 m long, and horizontal/vertical gauges.

Observations from our case study are organized in two time series for two vertical EL-beam displacement measurements. The time series represent a set of measurements or other statistics distributed at regular

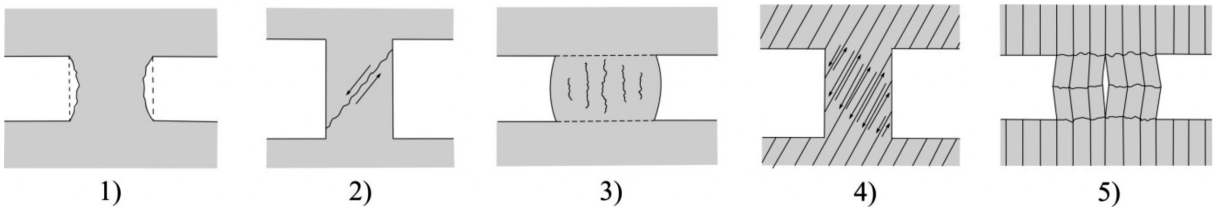

Figure 8. Different types of pillars discontinuities, remodelled from [17].

time intervals. One of the goals of time-series analysis is to make forecasts, i.e., to predict the future values of the tested statistics. The time series contain one or more of the following characteristics: trends, seasonal effects, cycles, and residuals.

To decompose the time series into the mentioned elements, we can use autoregressive (AR) or moving average (MA) processes, or a combination of the two. The AR process of order p is given by the equation:

$$X_t = \sum_{r=1}^{p} \beta_r X_{t-r} + \varepsilon_t \qquad (1)$$

with:

- β_r (r=1,p) – a set of constants,
- ε_t – a random variable.

The definition of the MA process of order q is:

$$X_t = \sum_{s=0}^{q} \xi_s \epsilon_{t-s} \qquad (2)$$

where ξ_s (s=0,q) is a set of constants and $\{\varepsilon_s\}$ is a series of uncorrelated random variables.

Combining models (1) and (2), the ARMA(p,q) process is obtained:

$$X_t - \sum_{r=1}^{p} \beta_r X_{t-r} + \varepsilon_t = \sum_{s=0}^{q} \xi_s \epsilon_{t-s} \qquad (3)$$

Model (3) applies for stationary processes. If the process is not a stationary one we integrate the original process by calculating the differences of d order, obtaining an autoregressive integrated process ARIMA (p,d,q). In order to discover the order of the AR and MA processes, as well as a possible order of differentiating, autocorrelation function (ACF) and partial autocorrelation function (PACF) are used in this case study.

3 RESULTS

3.1 Assumptions and starting conditions

The safety pillar, VS3 from Lipica II, has been monitored since 2010 (Fig. 9). In [13], the results of the observed open discontinuities of VS3 were discussed. The oversight was taken part for a period from October 2010 to June 2012. From a technical point of view, the EL beam gauge has been used as an optimal tool for high-safety--pillar stability monitoring. The EL beam gauge is easy to control in the case of technical failure. Its yearly control in a metrological laboratory is of great importance. Like other measuring equipment, its features and characteristics such as accuracy could vary in the changed environmental conditions [19]. In the case of vibrating-wire stress meters that were used in parallel, the correction or replacement is impossible due to the definitive fixation in a borehole with concrete.

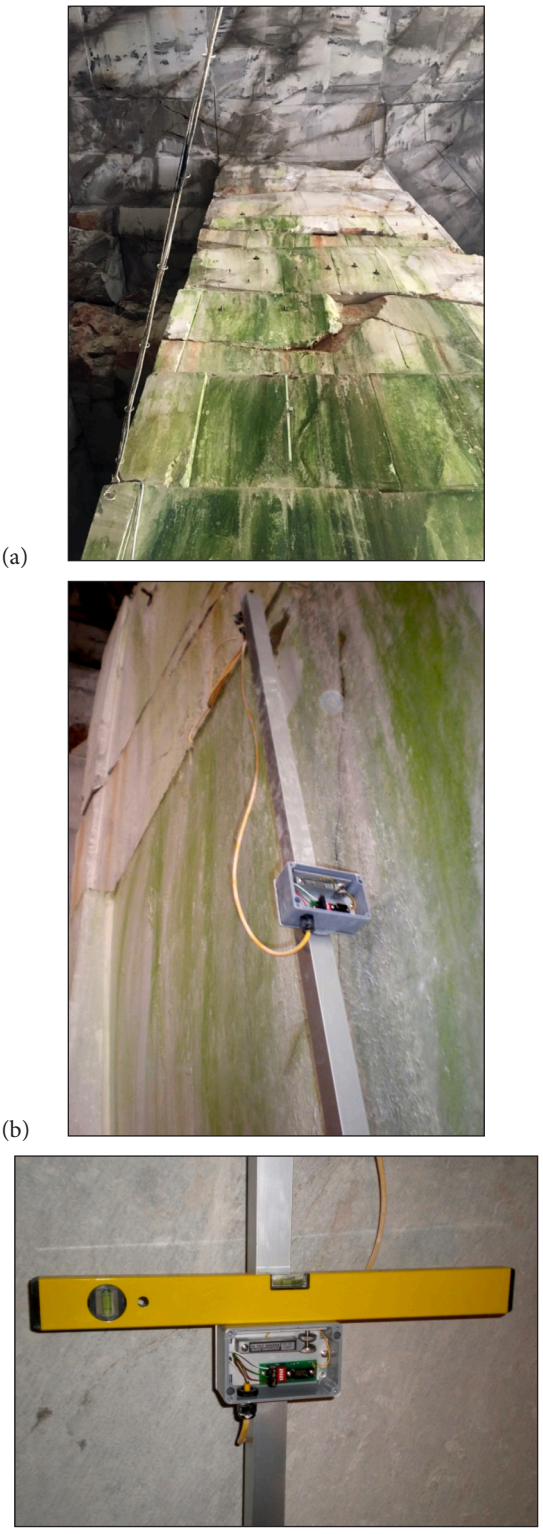

(a)

(b)

Figure 9. Safety Pillar VS3 (a) and Vertical EL beam gauge (b).

It was observed that the temperature has a huge impact on the metal rod of the EL beam gauge. That is why the temperature dataset, around the column, was collected during this monitoring of pillar VS3 where the 2-m-long datalogger was installed.

3.2 Measurements and results

The available dataset comprises the measured displacements with two vertically placed El-beams in the form of time series, covering the period April 2018 to April 2019. The measurements were performed on an hourly basis. The temperature measurements were also triggered for each measuring epoch in order to monitor the changes in the environmental conditions that could have an impact on the calculation of the trend lines for the displacements of the El beams.

The El-beam measurements for both beams are transformed to mm and put in Fig. 10. There are a few discrepancies in the dataset with the longest between 20-12-2018 and 14-1-2019.

It can be concluded from Fig. 10 that the measurements of the two El-beams (e_1 and e_2, respectively) are highly correlated. That is also numerically confirmed by the calculated correlation coefficient of 0.99. The same consideration applies to the dependency between the measurements and the temperature, having the correlation coefficients $r_{e_1,T} = r_{e_2,T} = 0.99$.

In order to test the changes in the El-beam lengths due to temperature we introduced a correction thermal expansion term. The applied El-beams are made of aluminium with a thermal expansion factor of 23.6 ppm/°C. After correcting the measurements for the influence of the ambient temperature, the corrected time series e_1' and e_2' were obtained. After the application of the correction for temperature, the El-beam measurements were still closely correlated with the temperature (r=0.99), meaning that the ambient temperature did not affect the instrumental characteristics. However, displacements do change in time due to changes in the temperature.

An analysis of the displacements was performed using ARMA modelling. To discover the order of the model, i.e., to find if there is a periodic behaviour of the time series, a test on autocorrelation was performed. To accomplish that we calculated the autocorrelation function (ACF). Since the ACF is only valid for stationary processes, and our dataset is not due to its variable standard deviation, we calculated the first-order differences for the whole dataset. The graphical result is depicted in Fig. 11.

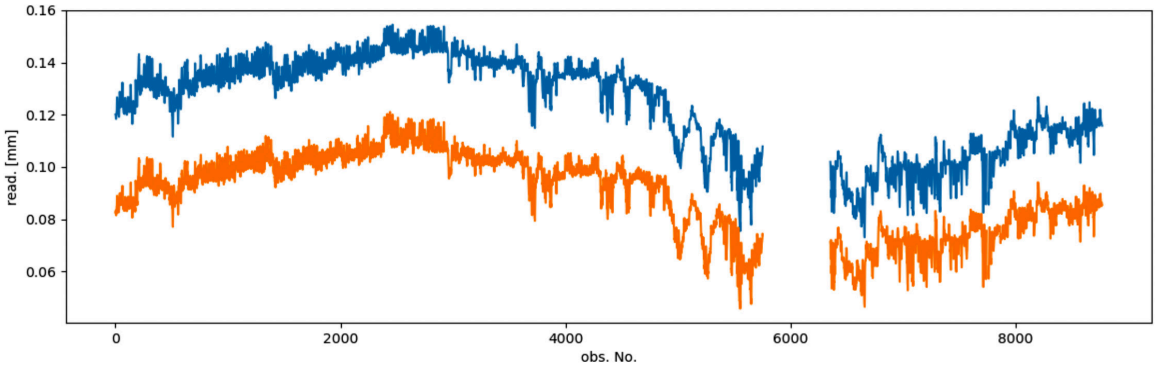

Figure 10. Measurements obtained from El-beams 1 and 2.

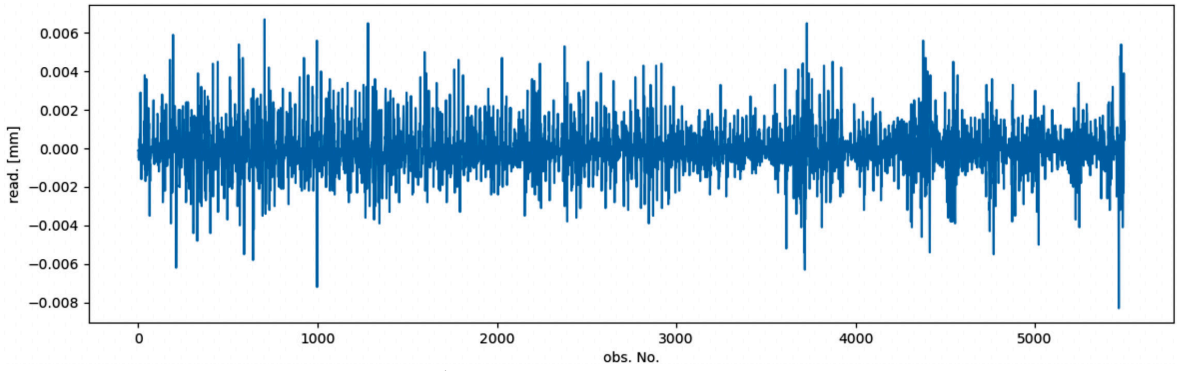

Figure 11. 1st-order differences for El-beam 1 time series.

Due to the discrepancies in the observation material, the rest of the analysis was performed for the period 24/5/2018 to 20/12/2018, containing the continuous observations. Also, due to the high correlation of El-beam 1 and El-beam 2, an ARMA prediction is performed with El-beam 1 only. In the case of the different behaviour of time series 1 and 2, the analysis of trends would be made with both El-beams, because the reason for such behaviour could be related to an uneven displacement of the pillars. The same stands for temperature measurements. The temperature was measured each hour. The high correlation between the temperature and the El-beam displacements means that hourly changes in the readings on El-beams are only due to the daily changes in temperature. Therefore, temperature measurements are still needed, in order to monitor the El-beam measurements and calculate the corrections for the temperature expansion.

The ACF graph is showed in Fig. 12. The shape of the graph and the observed periodic patterns in the form of a large spike at the first lag and more significant spikes with amplitudes of alternating sign at the further lags indicate that the dataset contains an autoregressive term

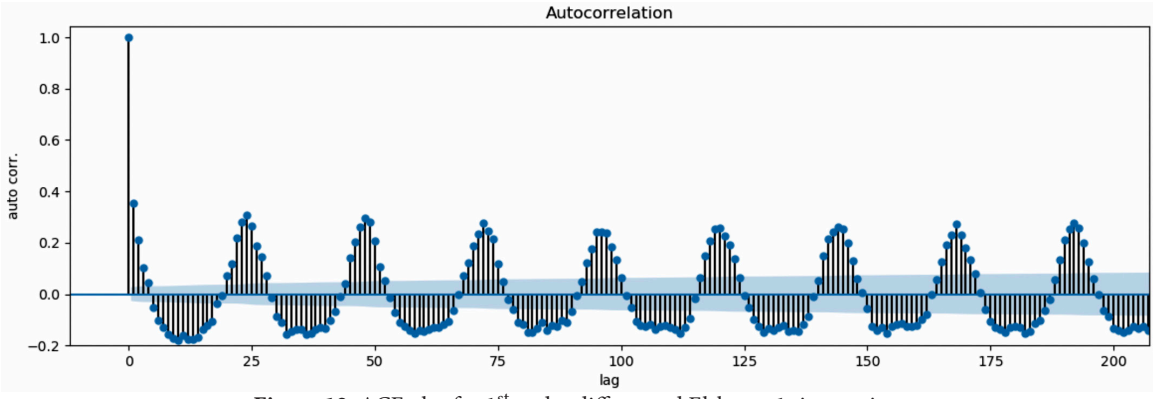

Figure 12. ACF plot for 1st-order differenced El-beam 1 time series.

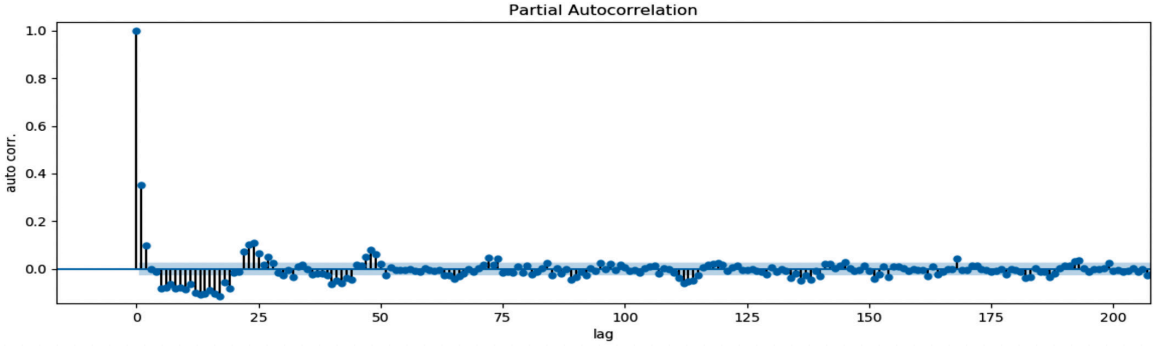

Figure 13. PACF plot for 1st-order differenced El-beam 1 time series.

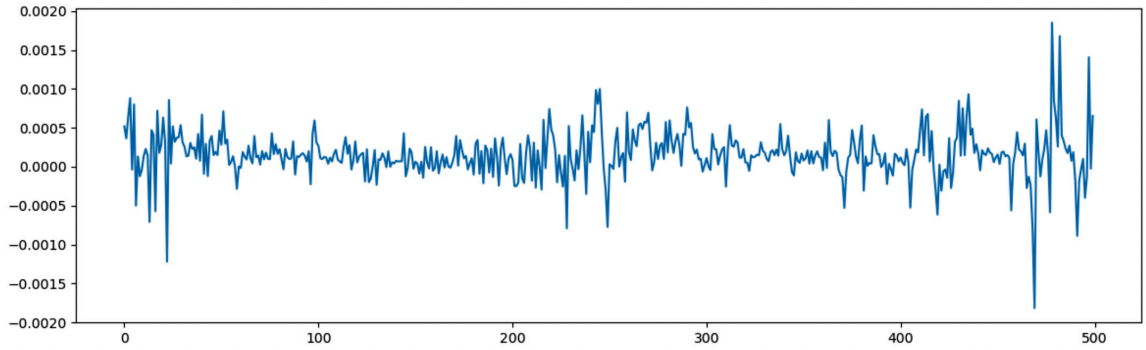

Figure 14. Differences between the 500 last predicted and original El-beam 1 readings.

of higher order. Due to the large dataset, only the first 200 lags are given in Fig. 3–4. The same pattern repeats for the rest of the dataset.

Determination of the order for the autoregressive term is made by calculating the partial autocorrelative function (PACF). The graphical representation of the result is presented in Fig. 13. Again, only the first 200 lags are shown because of the quantity of the processed data.

The obtained PACF results and the significant correlation only at the first lag with other correlations falling within the interval (-0.2; +0.2) suggests that the order of the AR coefficient is 1.

Analysing the ACF and PACF function graphs we performed the prediction with the ARMA(1,1) model. A test of the model congruence was made on the last 500 readings within the El-beam 1 dataset. A graphical representation of the differences is given in Fig. 14.

4 DISCUSSION

The graph in Fig. 14 represents the result of our study case. We used the whole available continual dataset as an input for our prediction model. Analysing the differences between the measured and predicted values given in Fig. 14, it can be concluded that all the predictions fall into the interval -0.002 to 0.002. Their values are $1/10^{th}$ of the measured values, which is negligible compared to the measurements themselves. In addition, there are no trends in the calculated differences. Therefore, the chosen model for the predictions is correctly chosen and applied [20, 21].

This model will be utilized in a sense to monitor, on daily basis, the values obtained using the ARMA prediction. The trend of predicted values should be smooth and within the proposed limits. The signal for some unusual events would be a sharp change in the trendline. In that case, certain actions should be taken. The whole process could be improved by automatically triggering alarms if the predicted values exceed certain given limits.

The applied dataset comprised a period of less than 1 year. From Fig. 10 it looks like a seasonal trend would occur. A longer time span of the observations should be included in the data processing to confirm this.

5 CONCLUSIONS

The observations used in this research consist of the measured displacements on two vertically placed El-Beams. Besides the linear discrepancies, the ambient temperatures were measured. Preliminary data processing showed, as expected, a significant correlation between both El-beams' measurements, as well as the temperatures correlated with the linear displacements, which was needed to investigate in more detail. The results of this analysis stage suggested there was no influence of the temperature on the El-beams, but rather on the stone itself.

In order to deal with possible dangerous situations that can occur in the case of the rapid displacements of rock blocks, we have developed a prediction model based on a time series of linear displacement measurements. The analysis of the observation material, its periodic characteristics and distribution over the time scale, showed that the ARMA(1.1) model describes the stochastic process the best. It resulted from the ACF and PACF plots created from the El-beam measurements.

In order to test the congruence of the calculated model, the predictions were made for 500 epochs, where real measured values already exist. The predictions showed a high level of congruence with the testing values, reflected in the calculated differences falling between -0.002 and 0.002, which is insignificant compared to the measurement accuracy of the El-beam. This result, therefore, proves the feasibility of the applied prediction model.

A longer observation period would also make possible the testing seasonal characteristics of the time series. Further work on this specific issue will include developing the automatic responding monitoring system, which would be triggered by warning events when the model reports sudden changes in the smoothness of the predicted values.

Acknowledgments

This research was supported by the Slovenian Ministry of Education Science and Sport, Faculty of Natural Sciences and Engineering, and research program P2 0268 financed by the Slovenian Research Agency. We would like to express our gratitude to Marmor Sežana d.d., who provided data. We would also like to thank the anonymous reviewers and members of the editorial team for their comments.

REFERENCES

[1] Jurkovšek, B., Biolchi, S., Furlani, S., et al 2016. Geology of the Classical Karst Region. J Maps 12,

352–362. https://doi.org/10.1080/17445647.2016.1215941
[2] Otoničar, B. 2000. Upper Cretaceous to Paleogene forbulge unconformity associated with foreland basin evolution (Kras, Matarsko Podolje and Istria; SW Slovenia and NW Croatia). Acta Carsologica 36, 101–120. https://doi.org/10.3986/ac.v36i1.213
[3] Kortnik, J. 2009. Underground natural stone excavation technics in Slovenia Tehnike podzemnega pridobivanja naravnega kamna v Sloveniji.
[4] Marmor Sežana Lipica II. http://www.marmorsezana.com/en/quarry/lipica-ii-quarry/. Accessed 19 Apr 2019.
[5] Natural Sciences. http://www.mstworkbooks.co.za/natural-sciences/gr9/gr9-eb-03.html. Accessed 19 Apr 2019.
[6] Lee, F.T., Abel, J.F. 1983. Subsidence from Underground Mining: Environmental Analysis and Planning Considerations. GEOLOGICAL SURVEY CIRCULAR 876. https://doi.org/10.3133/cir876
[7] Estrada-Medina, H., Graham, R.C., Allen, M.F., et al. 2013. The importance of limestone bedrock and dissolution karst features on tree root distribution in northern Yucatán, México. Plant Soil 362, 37-50. https://doi.org/10.1007/s11104-012-1175-x
[8] Chaulya, S.K., Chakraborty, M.K., Singh, R.S. 2001. Air Pollution Modelling for a Proposed Limestone Quarry. Water Air Soil Pollut 126, 171–191. https://doi.org/10.1023/A:1005279819145
[9] Neri, A.C., Sánchez, L.E. 2010. A procedure to evaluate environmental rehabilitation in limestone quarries. J Environ Manage 91, 2225–2237. https://doi.org/10.1016/J.JENVMAN.2010.06.005
[10] Kortnik, J. 2009. Optimisation of the high safety pillars for the underground excavation of natural stone blocks. Acta Geotech Slov 1, 34–48.
[11] Bogert, H., Jung, S.J., Lim, H.W. 1997. Room and pillar stope design in highly fractured area. Int J Rock Mech Min Sci. 34 (3,4), 145.e1-145.e14. https://doi.org/10.1016/S1365-1609(97)00155-X
[12] Lollino, G., Manconi, A., Guzzetti, F., et al. 2015. Engineering Geology for Society and Territory-Volume 5 Urban Geology, Sustainable Planning and Landscape Exploitation. https://doi.org/10.1007/978-3-319-09048-1_71
[13] Kortnik, J. 2015. Stability assessment of the high safety pillars in Slovenian natural stone mines. Arch Min Sci. 60, 403–417. https://doi.org/10.1515/amsc-2015-0027
[14] Fronteau, A., Lejeune, G., Sosson, O., et al. 2010. Influence of geomorphological constraints and exploitation techniques on stone quarry spatial organisation. Example of Lutetian underground quarries in Rheims. Laon Soissons areas Eng Geol 115, 268–275. https://doi.org/10.1016/j.enggeo.2010.05.004
[15] Biaxial Stressmeters | GEOKON, INCORPORATED. https://www.geokon.com/4350. Accessed 20 Apr 2019.
[16] EL Beam Sensor - DGSI - Durham Geo - Tiltmeters - Geotechnical Instrumentation. https://durhamgeo.com/product/el-beam-sensor/. Accessed 20 Apr 2019.
[17] Brandy,B.H.G., Brown, E.T. 2004. Rock mechanics for undeground mining. Springer Science, pp 372–380.
[18] Grasmueck, M. 1996. 3-D ground-penetrating radar applied to fracture imaging in gneiss. GEOPHYSICS 61, 1050–1064.
[19] Gučević, J., Delčev, S., Ogrizović, V. 2011. Determining Temperature Dependence of Collimation Error of Digital Level Leica DNA 03. In: FIG Working Week 2011, Bridging the Gap between Cultures, Marrakech, Morocco, 18-22 May 2011. FIG, Marrakech, Morocco, p 1.12.
[20] Kaluđerović, D., Koren, E., Vižintin, G. 2018. Application of analytic element method in hydrogeology. Mater Geoenvironment 65, 35–44. https://doi.org/10.1515/rmzmag-2018-0002
[21] Vižintin, G., Ravbar, N., Janež, J., et al. 2018. Integration of models of various types of aquifers for water quality management in the transboundary area of the Soča/Isonzo river basin (Slovenia/Italy). Sci Total Environ 619–620, 1214–1225. https://doi.org/10.1016/j.scitotenv.2017.11.017